Development of the Very Cold Neutron Source Prototype

Aleksenskii A.[1], Bleuel M.[2], Bosak A.[3], Dideikin A.[1], Dubois M.[4], Korobkina E.[5], Lychagin E.[6,7,8], Muzychka A.[6], Nekhaev G.[6], Nesvizhevsky N.[9], Nezvanov A.[6], Schweins R.[9], Strelkov A.[6], Turlybekuly K.[6], Vul' A.[1], and Zhernenkov K.[6,10]

[1] Ioffe Institute, St. Petersburg, Russia
[2] National Institute of Standards and Technology, Gaithersburg, USA
[3] European Synchrotron Radiation Facility, Grenoble, France
[4] SIGMA Clermont (ICCF), Université Clermont Auvergne, Aubière, France
[5] The University of North Carolina, Chapel Hill, USA
[6] Joint Institute for Nuclear Research, Dubna, Russia
[7] Lomonosov Moscow State University, Moscow, Russia
[8] Dubna State University, Dubna, Moscow reg., Russia
[9] Institut Max von Laue – Paul Langevin, Grenoble, France
[10] JCNS at Heinz Maier-Leibnitz Zentrum (MLZ), Forshungzentrum Julich GmbH, Garching, Germany

28th International Seminar on Interaction of Neutrons with Nuclei
May 24—28, 2021
online

Very Cold Neutrons (VCN)

UCN | CN

- the typical wavelengths are 2.5–60 nm;
- the velocities are 7–160 m/s;
- the energies are 0.25–130 μeV;
- the temperatures are 2.97×10^{-3}–1.55 K.

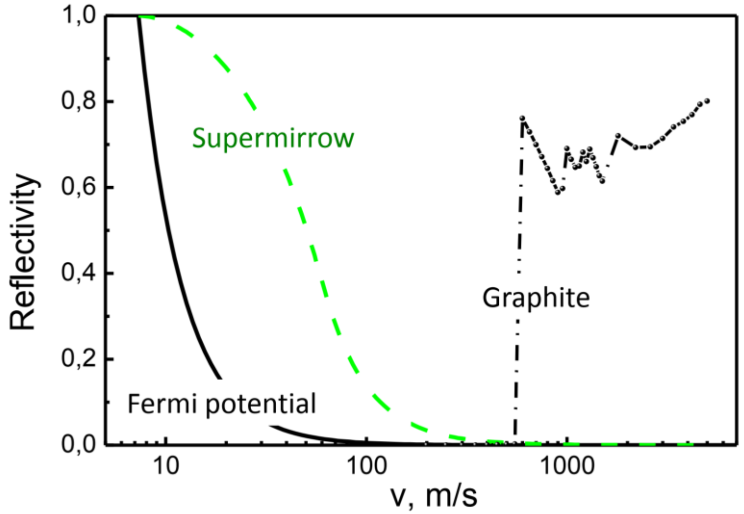

Fig. 1. The reflection probability for isotropic neutron flux.

Fig. 2. The scheme of the PF2 beam ports at the ILL, Grenoble, including the PF2/VCN platform.

This VCN beam is 7 cm high and 3.4 cm wide. The spectrum varies according to the height in the beam for v < 40 m/s, but is fairly homogeneous for v > 40 m/s.

The flux at v = 40 m/s (100 Å) is about 10^5 cm^{-2}s^{-1}(m/s)$^{-1}$ (= 0.4 x 10^5 cm^{-2}s^{-1}Å^{-1}).

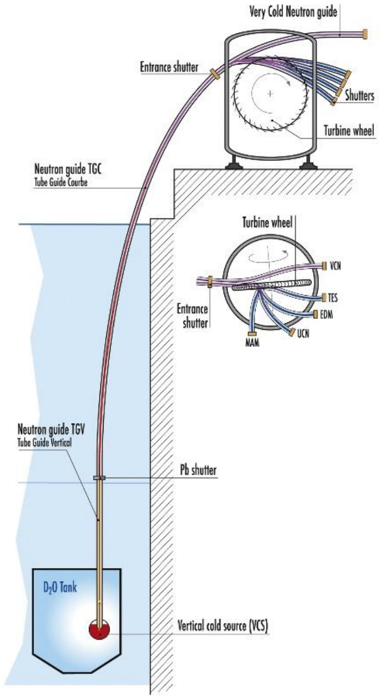

VCN Application

The VCN advantages are:
- long time of observation;
- large angles of reflections from mirrors;
- larger phase shift and as result more sensitive to contrast variation;
- large coherent length;
- large capture cross-section and big contrast at transmission;
- structure analysis of large molecular complexes; etc.

The main disadvantage is a low flux intensity!

Neutron techniques:
- SANS;
- spin-echo;
- TOF spectroscopy, in particular, high-resolution inelastic scattering;
- reflectometry, diffraction, microscopy, holography, tomography, etc.

Fundamental Physics:
- a search of extra-short-range interactions at neutron scattering;
- experiments with neutrons in a whispering gallery;
- beam experiment to measure of the neutron decay, etc.

Background

Articles about the VCN applications and prospects:

- R. Golub, “The production of very cold neutrons,” Physics Letters A, vol. 38, no. 3, pp. 177-178, 1972. DOI: 10.1016/0375-9601(72)90465-3
- V.V. Golikov, V.I. Lushchikov, and F.L. Shapiro, “Production of very cold neutrons,” JETP, vol. 37, no. 1, pp. 41-44, 1973. URL
- R. Gähler, A. Zeilinger, “Wave-optical experiments with very cold neutrons,” American Journal of Physics, vol. 59, no. 4, pp. 316-324, 1991. DOI: 10.1119/1.16540
- E.M. Rasel, K. Eder, J. Felber, R. Gähler, R. Golub, W. Mampe, and A. Zeilinger, “Interferometry with very Cold Neutrons”. In: van der Merwe A., Garuccio A. (eds) Waves and Particles in Light and Matter. Springer, Boston, MA. pp. 429-438, 1994. DOI: 10.1007/978-1-4615-2550-9_36
- G. van der Zouw, M. Weber, J. Felber, R. Gähler, P. Geltenbort, and A. Zeilinger, “Aharonov–Bohm and gravity experiments with the very-cold-neutron interferometer,” Nuclear Instruments and Methods in Physics Research A, vol. 440, no. 3, pp. 568-574, 2000. DOI: 10.1016/S0168-9002(99)01038-4
- R. Georgii, N. Arend, P. Böni, D. Lamago, S. Mühlbauer, and C. Pfleiderer, “Scientific Review: MIRA: Very Cold Neutrons for New Methods,” Neutron News, vol. 18, no. 2, pp. 25-28, 2007. DOI: 10.1080/10448630701328471
- V.V. Nesvizhevsky, “Reflectors for VCN and applications of VCN,” Revista Mexicana de Física S, vol. 57, no. 1, pp. 1-5, 2011. URL

Dedicated workshops:

- «Workshop on Applications of the Very Cold Neutron Source» 21-24 August 2005, Argonne National Laboratory, USA. URL
- «Present Status and Future of Very Cold Neutron Applications», 13-14 February 2006, Paul Scherrer Institute, Switzerland.
- «Very Cold Neutron Source for the Second Target Station Workshop», 27-28 April 2016, Oak Ridge National Laboratory, USA. URL

VCN Reflector

Criteria for the VCN reflector are minimum losses and maximum reflection.

Detonation nanodiamonds (DND) are the ideal candidate!

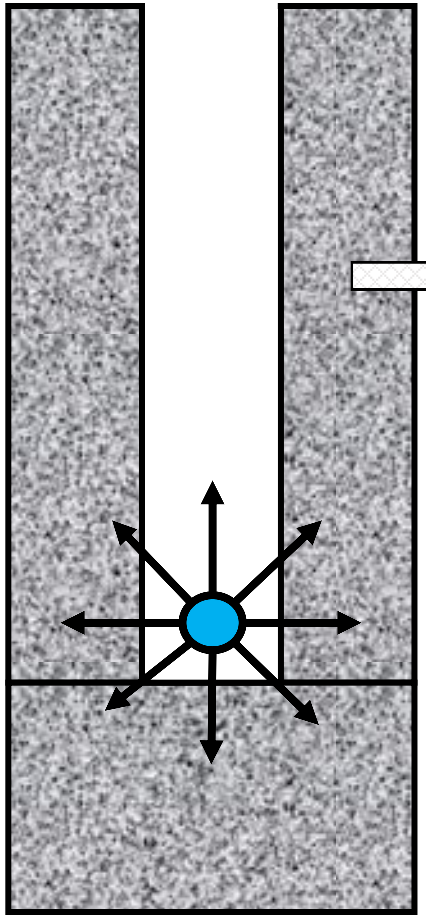

Fig. 2. The possible scheme of the VCN source.

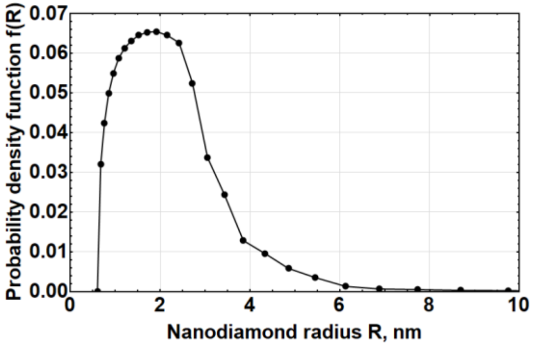

P_{REF}^{max}: $R_{opt} \approx 0.27\lambda$

$R_{opt}(\lambda) \approx 0.7 - 4.3\ nm$,
$\lambda \in [26, 160]$ Å
or $v \in [25, 150]\ m/s$

Positive Factors:

size distribution;
$b_{c.sc.}^{C} = 6.65\ fm$;
$\sigma_{c.sc.}^{C} = 5.55\ b$;
$\sigma_{abs}^{C} = 3.5\ mb$;
$\sigma_{in.sc.}^{C} \rightarrow 0\ (T \rightarrow 0)$;
$\rho^{Diamond} \approx 3.5\ g/cm^3$.

$P_{REF} \sim 95\%$

Negative Factors:

~10 at. % of hydrogen,
$\sigma_{abs}^{H} = 0.33\ b$;
$\sigma_{in.sc.}^{H} = 108 \pm 2\ b$;
other impurities
< 0.15 at. %

neutron capture — neutron activation

Implemented solutions:

the fluorination of DND
$C/H = 7.4 \pm 0.2$ (before)
$C/H = 430 \pm 30$ (after)

the additional purification of DND
$\Sigma_{abs}^{after}/\Sigma_{abs}^{before} \approx 0.58$
$\Sigma_{abs}^{H} \approx 0.2\Sigma_{abs}^{after}$
But still significant activation!

the deagglomeration of DND
$P_{REF}^{after}/P_{REF}^{before} \approx 1.10$
$\rho_{bulk}^{after}/\rho_{bulk}^{before} \approx 3$

Preliminary results!

Directional Extraction of VCN

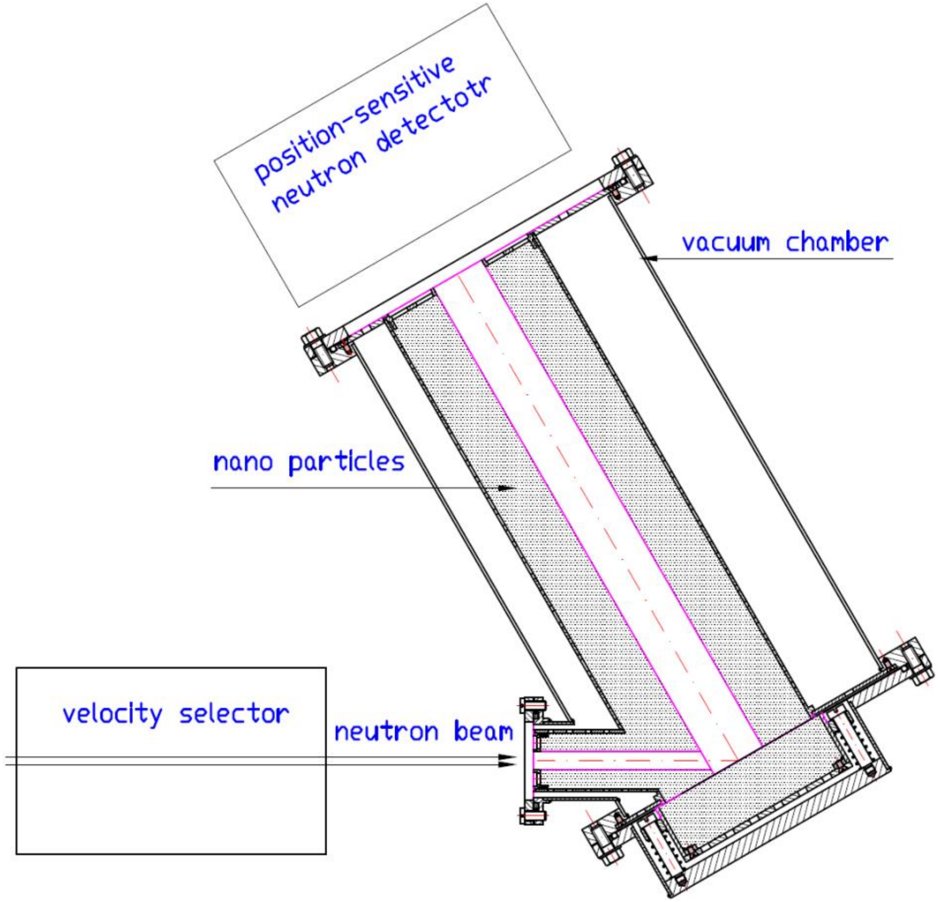

Fig. 3. The scheme of the experiment at the PF2/VCN, ILL, Grenoble (2017). Presented first during the ISINN-26.

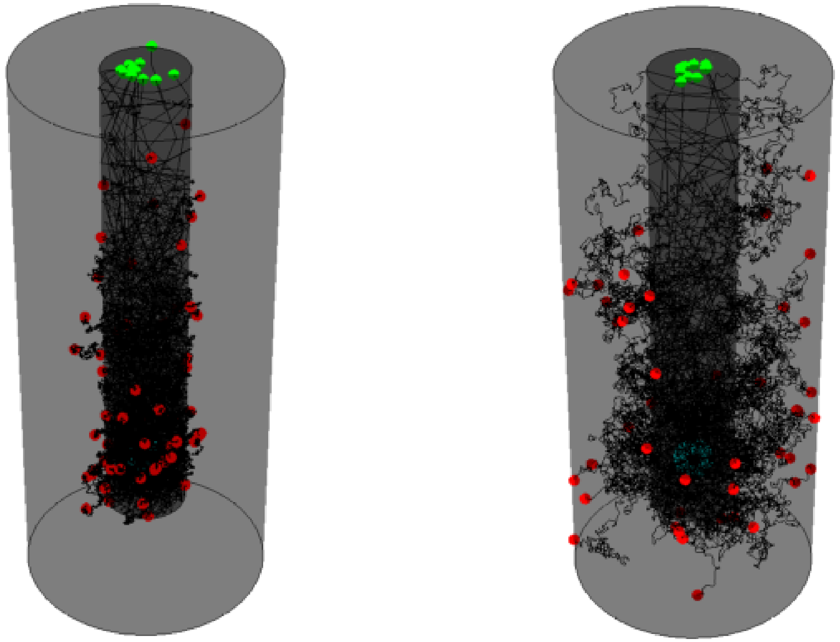

Fig. 4-5. Trajectory tracking for neutrons with velocities of 50 m/s (on left) and 100 m/s (on right) diffusing inside the fluorinated diamond nanopowder.

Preliminary experimental results: the neutron flux extracted to the exit hole was increased up to 10 times related to flux without the reflector.

The Idea of a VCN Source

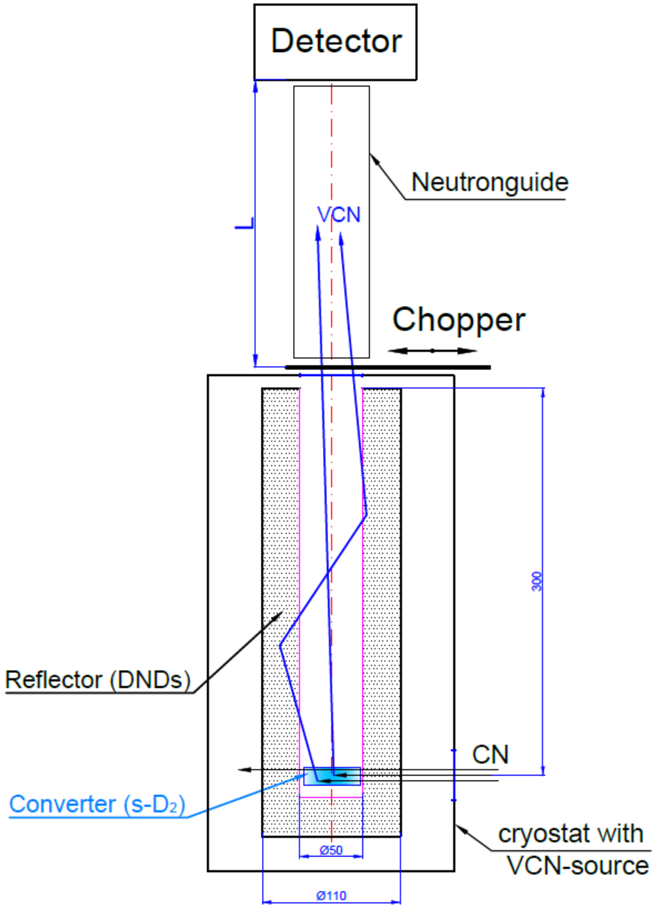

Fig. 6. The scheme of the upcoming demonstration of the VCN source prototype.

The converter tube is made from polytetrafluoroethylene (PTFE, Teflon™).

The inner diameter of the tube is 1 cm, the length is 5 cm, the wall thickness is 0.1 cm.

The temperature of solid ortho-deuterium is 5 K.

The reflector is a fluorinated deagglomerated diamond nanopowder (FD-DND). Its bulk density is 0.6 g/cm^3 and the mean size of a nanoparticle is 3 nm. The inner diameter of the cylinder is ≈5 cm, the height is 20-30 cm, the wall thickness is 1-3 cm.

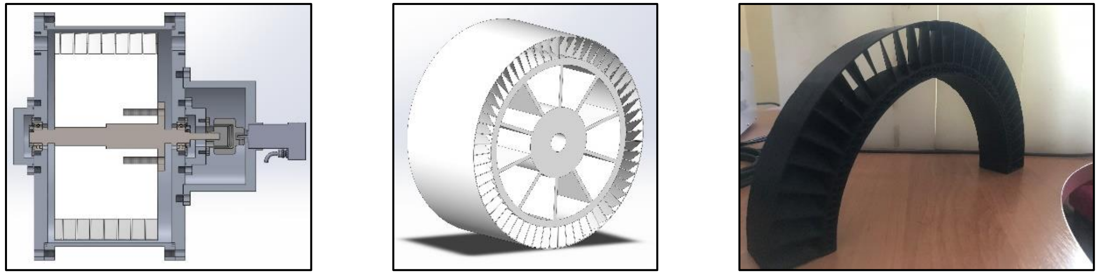

Fig. 7-9. The general scheme and the printed part of the optional velocity selector for VCN. It may be able to be used instead of the proposed chopper system.

Fig. 10. The first example of the PTFE cylinder with the converter tube.

Estimating the VCN Source Productivity

Unfortunately, there is no data on the VCN production!

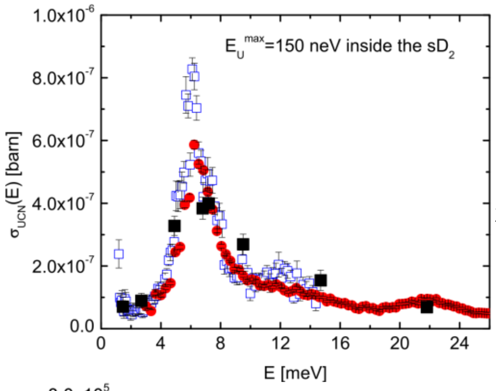

Fig. 11[1]. UCN production cross-section of c_o = 95.2% solid D_2. UCN energy range 0-150 neV inside the solid D_2. Cross-section determined by a integration of S(Q, E) along the free dispersion of the neutron (TS: "turbo-solid" - fast frozen solid deuterium (T =4 K)); data from IN4 measurements. Blue squares - E_0 =17.2 meV. Red filled circles - E_0 =67 meV. Black solid squares - data from measurements at the PSI.

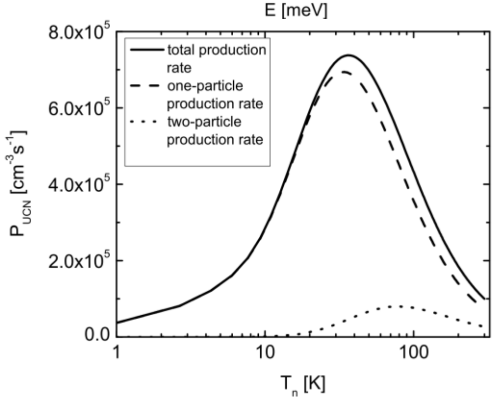

Fig. 12[1]. Calculated UCN production rate of c_o = 98% solid D_2 for different Maxwellian neutron spectra (effective neutron temperature T_n). UCN energy range - 0-150 neV inside the solid D_2. Neutron capture flux $\Phi_C = 1 \cdot 10^{14}$ cm^{-2} s^{-1}. Dashed line - one-particle production rate. Doted line - two-particle production rate. Solid line - total production rate.

VCN production cross-section approximation: $\sigma_{VCN} = \sigma_{UCN}\left(\frac{V_{VCN}}{V_{UCN}}\right)^3$, $V_{UCN} = 5.4\ m/s$ (150 neV); $[0, V_{VCN}]$ m/s – the VCN production range.

The converter volume is ≈ 4 cm^3.

Maxwellian spectrum of cold neutrons: $v_n^{mode} = 1000\ m/s$ ($T_n = 60\ K$).

Flux density is $J_0 = 10^{10}\ n/cm^2/s$.

VCN Production Rate

$[0,50]\ m/s$: $\Phi_{VCN}(50) = 1.6 \times 10^6\ n/s$;

$[0,100]\ m/s$: $\Phi_{VCN}(100) = 2.0 \times 10^6\ n/s$.

Attenuation Factors

"Useful" VCN limited by $v_n^{\rightarrow} = 6\ m/s$: $P_\Omega(50) \approx 4 \times 10^{-3}$; $P_\Omega(100) \approx 1 \times 10^{-3}$.

The duty cycle of the chopper disk: 10^{-2}

Expected Flux on the Detector

$$\boldsymbol{\Phi_{det}(50) = 8\ n/s;}$$
$$\boldsymbol{\Phi_{det}(100) = 16\ n/s.}$$

Estimating the Losses in the VCN Source with a Reflector

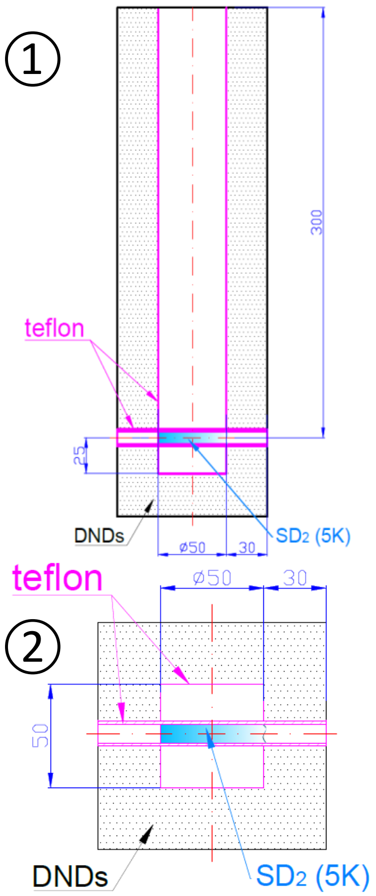

Fig. 13-14. Different source geometries for losses estimation.

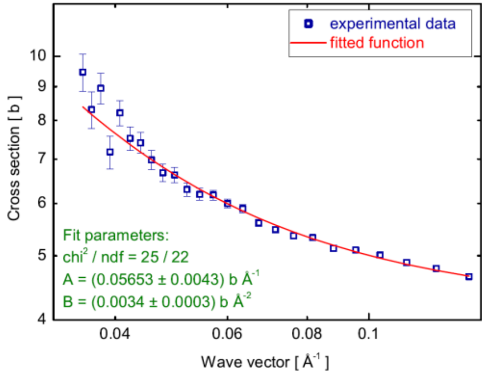

Fig. 15[2]. Total losses cross-section for the VCN in the s-D_2 (T = 5 K).

The case of our source:

$$\sigma_{loss}^{D_2} = \frac{A}{k}$$

$$\sigma_{loss}^{D_2}(50) = \frac{0.0565}{0.078} = 0.72\ b;\ \sigma_{loss}^{D_2}(100) = \frac{0.0565}{0.156} = 0.36\ b;$$

$$\boldsymbol{P_{loss}^{D_2}(50) = 2.8 \times 10^{-3}; P_{loss}^{D_2}(100) = 1.4 \times 10^{-3}.}$$

It is convenient to consider geometry ② for the losses estimation:

- the reflector's bottom is the main source of the "useful" VCN;
- if the albedo is ~90% the bottom volume will have almost isotropic VCN.

The cavity in such geometry ② will have the maximum flux.

Losses per flight through the cavity (≈ → =)

$V_0 = 98\ cm^3$ - the cavity volume; $S_0 = 118\ cm^2$ - the cavity area.
$l_0 = 4V_0/S_0 = 3.3\ cm$ – the mean free path of a VCN in the cavity;
$V_D = 4\ cm^3$- the s-D_2 volume; $\rho_D = 0.2\ g/cm^3$ - the s-D_2 density;
$l_D = l_0 V_D/V_0 = 0.13\ cm$ – the VCN mean free path in the s-D_2.

$V_w = 2.4\ cm^3$ - the PTFE volume in the walls;
$V_t = 1.7\ cm^3$ - the PTFE volume in the converter tube;
$V_{PTFE} = 2V_w + V_t = 6.5\ cm^3$ - the total PTFE volume;
$l_{PTFE} = l_0 V_{PTFE}/V_0 = 0.22\ cm$ - the VCN mean free path in the PTFE; $\rho_{PTFE} = 2.2\ g/cm^3$ - the PTFE density;
$\sigma_{loss}^{CF_2}(50) = 1.0\ b;\ \sigma_{loss}^{CF_2}(100) = 0.5\ b;$

$$\boldsymbol{P_{loss}^{PTFE}(50) = 6 \times 10^{-3};}$$
$$\boldsymbol{P_{loss}^{PTFE}(100) = 3 \times 10^{-3}.}$$

The converter tube creates two holes in the reflector. They can totally absorb neutrons in the worst-case.
$S_{hole} = 1.1\ cm^2$ - the hole area;

$$\boldsymbol{P_{loss}^{holes} = 2S_{hole}/S_0 = 1.9 \times 10^{-2}.}$$

Monte-Carlo simulation of the VCN reflection from the FD-DND in geometry #2 gives us:

$$\boldsymbol{P_{loss}^{FD-DND}(50) = 4 \times 10^{-2};}$$
$$\boldsymbol{P_{loss}^{FD-DND}(100) = 1.5 \times 10^{-1}.}$$

Estimating the Efficiency of the Reflector

The gain factor G of the VCN flux due to the usage of the proposed VCN reflector: $G \sim \frac{1}{P_{loss}}$

	$50\ m/s$	$100\ m/s$
$P_{loss}^{D_2}$	2.8×10^{-3}	1.4×10^{-3}
P_{loss}^{PTFE}	6.0×10^{-3}	3.0×10^{-3}
P_{loss}^{holes}	1.9×10^{-2}	1.9×10^{-2}
P_{loss}^{FD-DND}	4.0×10^{-2}	1.5×10^{-1}
Total losses P_{loss}^{min}	$\sim\mathbf{6.8 \times 10^{-2}}$	$\sim\mathbf{1.7 \times 10^{-1}}$

Table 1. List of all possible losses.

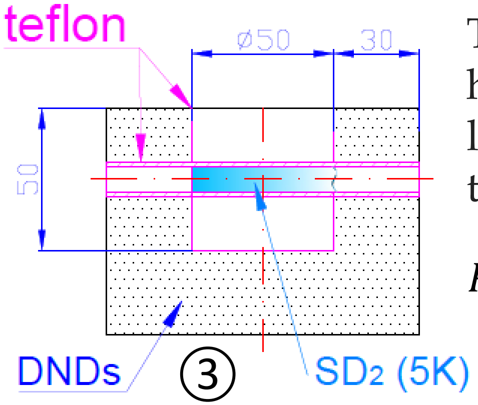

The geometry ③ has the maximum losses comparing to the others:

$$P_{loss}^{max} = P_{loss}^{min} + P_{loss}^{top},$$
$$P_{loss}^{top} = 1.6 \times 10^{-1}.$$

$$G_{max} \sim \frac{1}{P_{loss}^{min}}: \ G_{max}(50) \sim 15; \ G_{max}(100) \sim 6;$$
$$G_{min} \sim \frac{1}{P_{loss}^{max}}: \ G_{min}(50) \sim 4; \ G_{min}(100) \sim 3.$$

Accordingly, the expected neutron flux $\Phi'_{det}(V_{VCN})$ to the detector in the geometry ① with the reflector:

$$\Phi'_{det}(V_{VCN}) \in [\Phi_{det} \cdot G_{min}, \Phi_{det} \cdot G_{max}]$$

$$\boldsymbol{\Phi'_{det}(50) = 32 - 120\ n/s;}$$
$$\boldsymbol{\Phi'_{det}(100) = 48 - 96\ n/s.}$$

Models and Simulation

<u>New Approach</u>
for the extracting nanopowder parameters. Software "Structural Nanopowders Analyzer Based on Small-Angle Scattering Data (SNASAS)", RU2020662675.
Its allows us to observe and to estimate the effect of nanopowder modification, for instance, deagglomeration and separation. As well as to compare the reflectivity of such nanopowders.

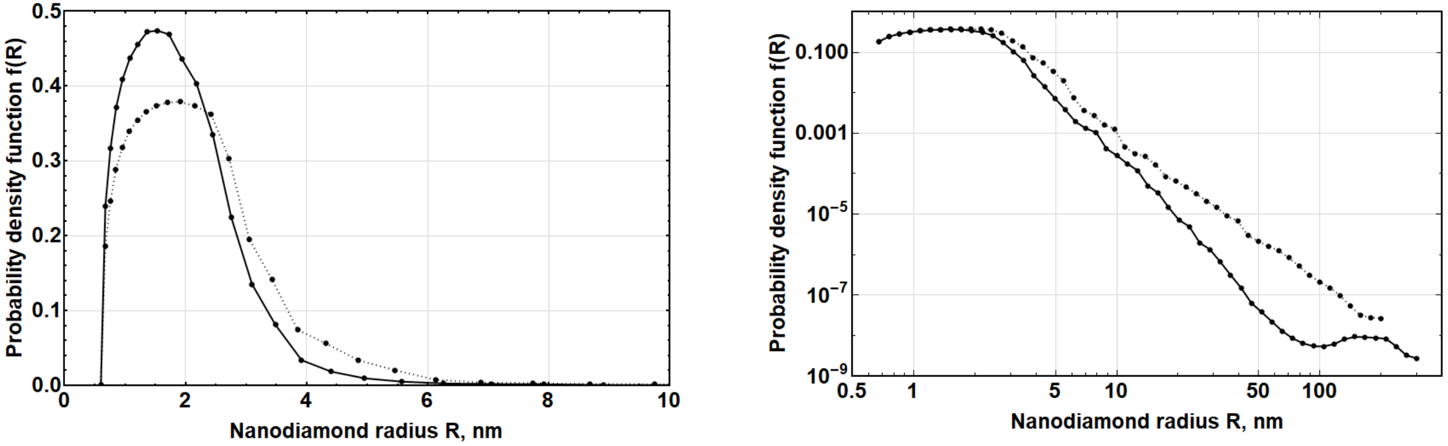

Fig. 16-17. Size distributions of the fluorinated DND (F-DND, dotted) and the FD-DND (solid).

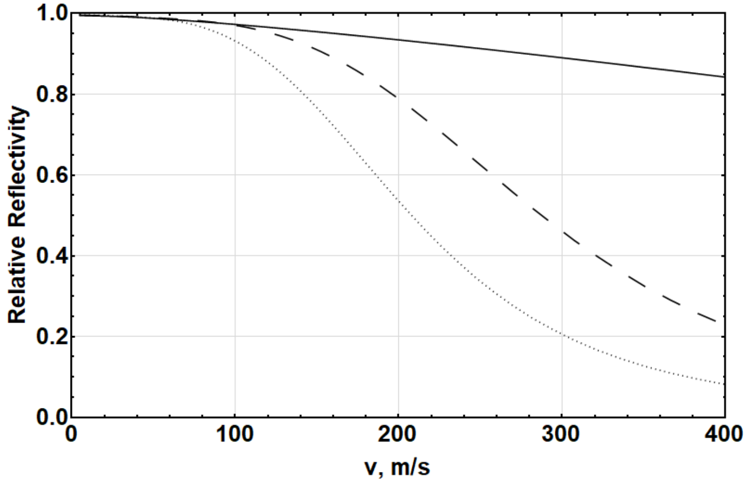

Fig. 18. The relative reflectivity of the 3 cm thick F-DND layer (dotted), FD-DND (dashed) and the infinity cm thick FD-DND layer (solid line).

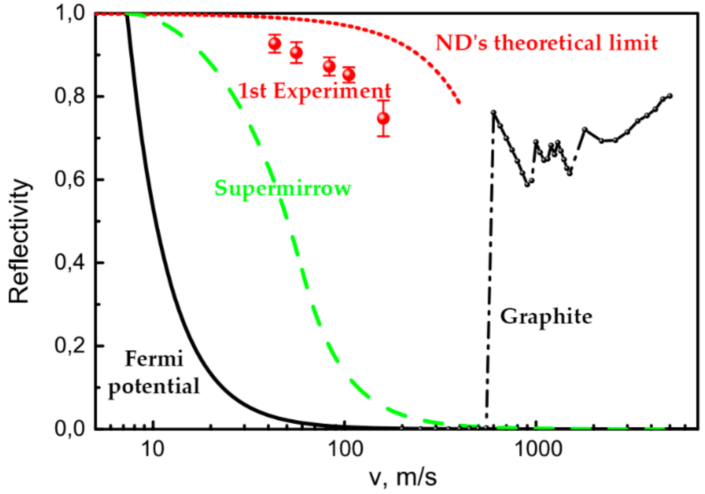

Fig. 19. The reflection probability of neutrons with the data for the non-fluorinated DND.

The absolute reflectivity of the F-DND must be much better than in the 1st experiment with the raw nanopowder.

Therefore, the reflectivity of the FD-DND is already near to the theoretical maximum!

Close Future Plans

- The designing and developing of the vacuum and cooling systems.
- Finishing the study of the PTFE converter tube and the reflector walls.
- Testing the assembly at the IBR-2, Dubna.
- To continue the development of the VCN selector.
- Monte-Carlo simulation:
  - different modified nanopowders;
  - different geometries of the reflector;
  - the model integration to the Geant4 code;
  - the undiscribed experimental data of the directional VCN extraction and the quasi-specular reflection of cold neutrons.
- The final test of the prototype at the PF1B cold neutron beam at the ILL approximately in 2024.

Thank you all for your kind attention!

This research was funded by grants
RFFI-18-29-19039, ERC INFRASUP P-2019-1/871072, and CREMLINplus grant agreement 871072.

The authors are grateful to V. Artem'ev, C. Hramco, O. Ivankov, K. Kornieieva, O. Kristavchuk, M. Mikhaylov, O. Orelovich.

Alexander NEZVANOV, Ph.D.
nezvanov@jinr.ru
Frank Laboratory of Neutron Physics
Joint Institute for Nuclear Research, Dubna.